Inhibition Behavior of Chito-Oligosaccharide Schiff Base Derivatives for Mild Steel in 3.5% NaCl Solution

Fubin Ma[1, 2], Weihua Li[1,*], Huiwen Tian[1], Qinglin Kong[3], Baorong Hou[1]

[1] Institute of Oceanology, Chinese Academy of Sciences, Qingdao 266071, China
[2] University of Chinese Academy of Sciences, Beijing 100049, China
[3] University of Melbourne, Melbourne 3010, Australia
[*]E-mail: liweihua@qdio.ac.cn

Two new corrosion inhibitors of chito-oligosaccharide schiff base (CSB) and carboxymethyl chito-oligosaccharide schiff base (CM-CSB) were investigated by means of weight loss, potentiodynamic polarization and electrochemical impedance spectroscopy (EIS) measurements in 3.5% NaCl solution at different concentrations. The surface corrosion morphology of specimens was examined by scanning electron microscopy (SEM) and the inhibition mechanism was analyzed by adsorption isotherm fitting and quantum chemical calculation. The results showed that for CSB the inhibition efficiency increased at first, then decreased and reached the maximum at 200mg/L and acted as a mixed type inhibitor; the CM-CSB had excellent inhibition performance and behaved as a cathode-based mixed corrosion inhibitor. The adsorption of CM-CSB obeys the Langmuir isotherm.

1. INTRODUCTION

Seawater is used in many areas such as cooling systems, storage reservoirs, and water pipelines for injection systems, but it inevitably causes corrosion problems. Application of inhibitors is a simple but effective method for protection of materials against corrosion[1−3]. Many inorganic inhibitors such as chromates, phosphates, hypophosphates, alkalis, nitrite and fluorides have been widely studied[4-6]. However, some inhibitors have adverse effect on the environment. Thus organic inhibitors of great potential as an alternative to the adverse inorganic inhibitors have been the focus of researchers[7-11].

Chito-oligosaccharide is the degradation products of chitosan (n=2~10). Due to its good water solubility and distinct biological activity, it is widely used in the fields of medicines, foods, cosmetics

and so on[12-14]. Schiff base compounds are condensation products of amines and ketones/aldehyde. Recent publications have showed increasing attention to these compounds as corrosion inhibitors in typical acidic environment for various metals such as mild steel, aluminum and copper[15–21]. Schiff base ligands have significant importance in chemistry, especially in the formation of Schiff base complexes, because Schiff base ligands are capable of forming stable complexes with metal ions[22], which are of great potential in corrosion and protection area.

The aim of this study is to investigate the inhibition effect of two chito-oligosaccharide derivatives -- chito-oligosaccharide schiff base (CSB) and carboxymethyl chito-oligosaccharide schiff base (CM-CSB) -- on the mild steel in 3.5% NaCl solution through weight loss, potentiodynamic polarization and electrochemical impedance spectroscopy (EIS) measurements. The surface corrosion morphology was examined by scanning electron microscopy (SEM) and the inhibition mechanism was analyzed by adsorption isotherm fitting and quantum chemical calculation.

2. EXPERIMENTAL

2.1 Materials and specimens preparation

Chito-oligosaccharide schiff base (CSB) and carboxymethyl chito-oligosaccharide schiff base（CM-CSB）compounds were synthesized by Qingdao University of Science and Technology. The molecular structures are shown in Figure 1. The test solutions were 3.5% NaCl solution prepared from reagent grade chemicals and double-distilled water with/without inhibitors. The concentration of the inhibitors ranged 100mg/L to 800mg/L and solutions without inhibitor were used for blank experiment. The specimens were cut from the mild steel with the chemical composition (wt %): 0.17 C, 0.46 Mn; 0.26 Si; 0.017 S; 0.019 Cu, and Fe in balance.

Figure 1. molecular structures of CSB and CM-CSB

2.2 Weight loss measurements

Specimens used in the weight loss experiment were mechanically cut into 50.0mm×25.0 mm×4.5 mm, then polished in sequence with a series of emery paper (grade 80, 240, 600, 800) washed

with distilled water, degreased in acetone and ultrasonically cleaned in alcohol. After dried in desiccator and weighed accurately, they were immersed in breakers containing 350ml 3.5% NaCl solutions without/with different concentrations of inhibitors (100mg/l, 200mg/l, 400mg/l, 600mg/l, 800mg/l) for 15 days. Then they were taken out, washed with distilled water, ultrasonically cleaned in alcohol, dried in desiccator and weighed accurately by analytical balance. The average weight loss of each group for three parallel specimens was obtained.

2.3 Surface observation and analysis

The mild steel specimens with the dimension of 10.0 mm×10.0 mm ×10.0 mm were roughened down to 2.5μm and washed with distilled water and acetone. The surface corrosion morphologies of specimens after immersing for 15 days in 3.5% NaCl solution with 200mg/L CSB and 800mg/L CM-CSB were obtained on a KYKY2800B scanning electronic microscope. The accelerating voltage was 25 kV.

2.4 Electrochemical experiments

The mild steel specimens used as working electrode were embedded in epoxy resin with an exposed surface area of $1cm^2$. The treatment of the working surface was the same as described in Section 2.2. The counter electrode was a platinum plate (15.0mm×15.0mm) and the reference electrode was a saturated KCl calomel electrode (SCE) coupled with a Luggin capillary. The electrochemical experiments were carried out with a PARSTAT 2273 Potentiostat/Galvanostat in non-deaerated solutions at 298±2K. An electrochemical cell with a three-electrode configuration was connected to PARSTAT 2273 Potentiostat/Galvanostat (Princeton Applied Research) which was shown in Figure 2.
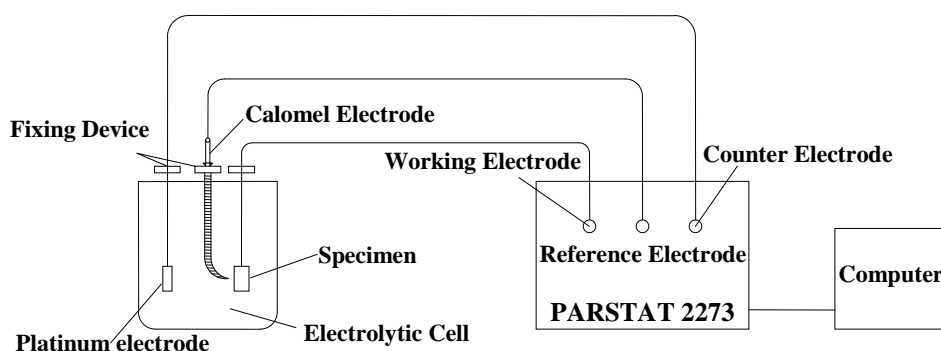
Figure 2. Electrochemical measurement system

The working electrode was immersed in 3.5% NaCl solution until a steady-state open-circuit potential (OCP) was obtained. The poentiodynamic polarization curves were recorded from −250mV to +250mV (vs. OCP) with a scanning rate of 0.5 mV s^{-1} and the data were collected and analyzed by

electrochemical software PowerSuite ver.2.58. EIS measurements were carried out at steady state open circuit potential (OCP) with amplitude of 10 mV ac sine wave. The frequency range was 100 kHz-10 mHz. The impedance data were analyzed and fitted using ZSimpWin ver.3.21.

2.5 Quantum chemical calculation

For further understanding of the interactions between the inhibitor molecules and the specimen surface, molecular simulation and quantum chemical study were performed by Hyperchem 7.5 software. The structure of the molecular was fully geometrically optimized by the method of PM3 in Semi-empirical way.

3. RESULTS AND DISCUSSION

3.1 Weight loss measurement

Weight loss measurement is a useful method of evaluating inhibition efficiency. The inhibition efficiency was evaluated by Eq. (1).

$$IE_w\% = \frac{W^0 - W}{W^0} \times 100 \qquad (1)$$

Where W^0 and W were the corrosion rates in the absence and presence of inhibitors, respectively. The results of weight loss measurement with the inhibitors of 0, 100, 200, 400, 600, 800mg/L in 3.5% NaCl solutions were shown in Table 1.

Table 1. Efficiency of the CSB and CM-CSB calculated from weight loss measurement

Concentration/(mg/L)		100	200	400	600	800
IE/%	CSB	43.31	70.63	64.09	51.42	30.42
	CM-CSB	31.62	46.38	56.73	62.69	76.84

The results as shown in Table 1 showed that the corrosion rate of the CSB on mild steel increased first, then decreased and the maximum inhibition efficiency was achieved at 200mg/L. The reason may be that with the increasing of the CSB concentration the water-solubility reduces, meanwhile protective film formed by CSB molecules were less compact which leads local corrosion[24]. The desorption speed is higher than the adsorption speed. It also can be observed that inhibition efficiency of the CM-CSB reached 76.84 % indicating that the CM-CSB has better inhibition effect compared with CSB. The reason is that carboxymethyl molecular modification improves its water solubility and makes the molecule richer in -NH$_2$ 、-COOH、-CH=NH groups

which contribute to the formation of a co-ordinate type of bond between Fe atoms and lone pair of electrons present in the inhibitors. Based on these reasons, the compactness and integrity are better when concentration increases.

The highest inhibition efficiency attained by weight loss experiment was on the boundary of the experiment. Theoretically, it should expand the experimental scope and seek the higher inhibition efficiency, but when the concentrations are over 1000mg/L, the practical application significance is limited, therefore, 800mg/L is appropriate[25].

3.2 Potentiodynamic polarization measurement

Figure 3 shows typical polarization curves of the CSB and CM-CSB.

a. CSB   b. CM-CSB
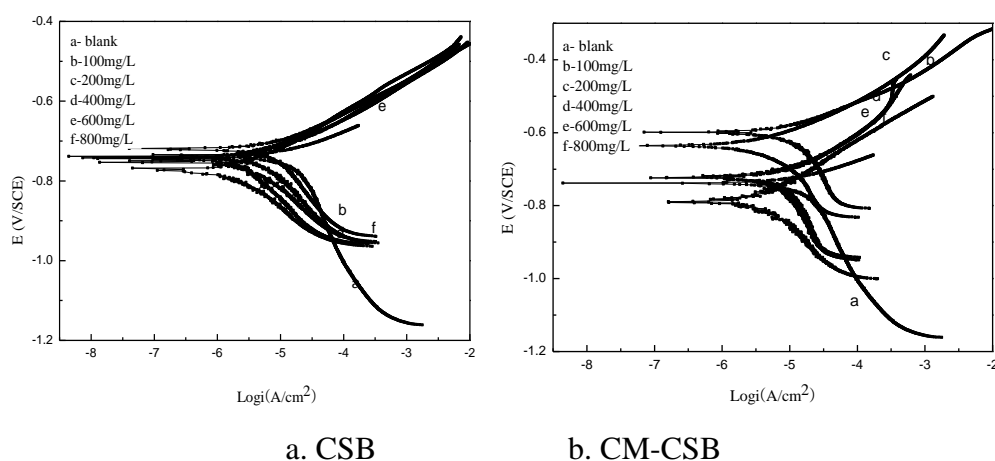
Figure 3. Polarization curves for mild steel in 3.5% NaCl solution

Figure 3.a shows that all the anodic polarization curves are parallel, which suggests the inhibitor don't affect the anodic reaction mechanism. After adding inhibitors, E_{corr} moves to a lower value, and the β_a and β_c decrease. It can be indicated that CSB acts as a mixed-type inhibitor. Figure 3.b shows that the current densities decrease sharply with the presence of the inhibitor, which suggests that compounds adsorb on the surface therefore suppressing the cathodic reaction (oxygen reduction) and anodic reaction (metal dissolution). As shown in Figure 3 that the anodic curves shift towards positive potential region at the low concentration, however, the curves shift negatively as the concentration increases. Generally when the change of corrosion potential is over 85mv, the corrosion inhibitor is thought to be a cathodic or anodic type inhibitor. Therefore, CM-CSB behaves as cathode-based mixed corrosion inhibitor[26] . The inhibition efficiency of CM-CSB reached the maximum value of 81.90% at 800mg/L, which agrees with weight loss results.

Electrochemical parameters such as corrosion current density (I_{corr}), corrosion potential (E_{corr}), Tafel constants β_a and β_c, and inhibition efficiency (IE) are calculated from Tafel plots and given in Table 2. The inhibition efficiency was calculated from Eq. (2)[27]:

$$IE\% = \frac{i^o_{\,corr} - i_{corr}}{i^o_{\,corr}} \times 100 \qquad (2)$$

where i_{corr} and $i^0_{\,corr}$ are the corrosion current densities with and without inhibitor.

Table 2. Polarization parameters for mild steel in 3.5% NaCl at 298K

inhibitor	C/(mg/L)	E_{corr} / mV	I_{corr} /uA cm^{-2}	βc /mV	βa /mV	IE /%
blank	0	-723.8	14.240	363.8	82.14	----
CSB	100	-713.9	8.273	244.7	109.4	41.90%
	200	-778.0	4.286	199.3	66.1	69.90%
	400	-741.8	6.797	224.6	61.0	52.27%
	600	-745.6	6.862	232.9	62.3	51.81%
	800	-733.4	7.441	156.0	61.4	47.75%
CM-CSB	100	-593.3	6.897	343.163	102.15	51.57%
	200	-621.5	5.802	252.527	161.73	59.25%
	400	-712.1	4.754	669.108	106.20	66.61%
	600	-715.8	4.311	618.022	117.67	69.73%
	800	-697.4	2.578	623.509	115.64	81.90%

It can be seen from the table that for CSB by increasing inhibitor concentration, the corrosion rate decreased and then increased with the same trend with inhibition efficiency. Moreover, the CSB causes little change in the anodic and cathodic Tafel slopes, indicating that the inhibitors firstly adsorb onto the surface and impede the reaction by merely blocking the reaction sites of iron surface without affecting the anodic and cathodic reaction mechanism[28]. However, it is also evident that the values of cathodic tafel slope ($\boldsymbol{\beta}_c$) and anodic tafel slope ($\boldsymbol{\beta}_a$) of the CM-CSB changed greatly which indicates that the inhibitor affects both the anodic and cathodic reactions. However, compared with the blank solution the cathodic tafel slope ($\boldsymbol{\beta}_c$) has greater change, so CM-CSB behaves as cathode-based mixed corrosion inhibitor. The cathodic reaction is the depolarization process of oxygen and the corrosion of carbon steel is controlled by the cathodic reaction; CM-CSB compounds form a film on the surface which reduces the diffusion rate of oxygen and suppresses the cathodic reaction thus showing good inhibition effect.

3.3 Electrochemical impedance spectroscopy (EIS)

The effects of the CSB and the CM-CSB on the impedance behavior of steel in 3.5% NaCl solutions are given in Figure 4. The fitted data shown in Table 4 follows almost the same pattern with the experimental results with R(Q(R(QR))) equivalent circuit is shown in Figure 5.
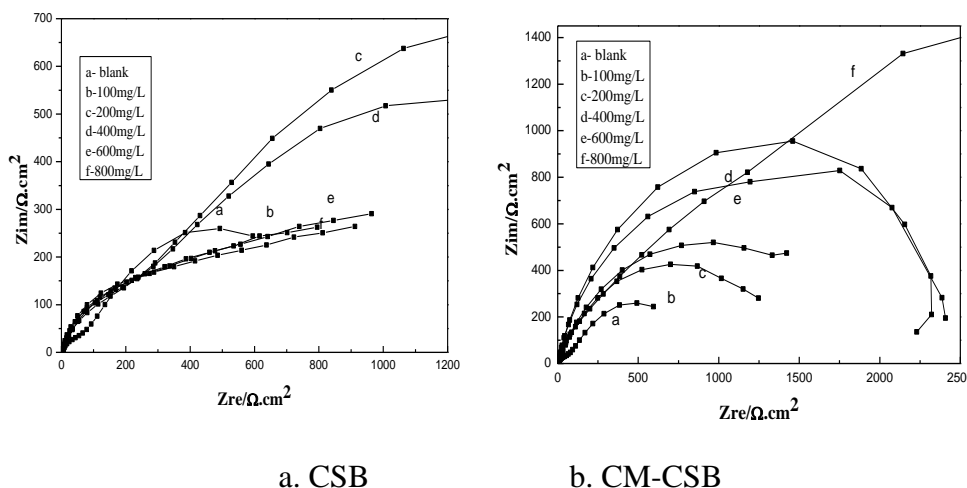
a. CSB   b. CM-CSB

Figure 4. Nyquist plots of CSB and CM-CSB for mild steel in 3.5% NaCl solution
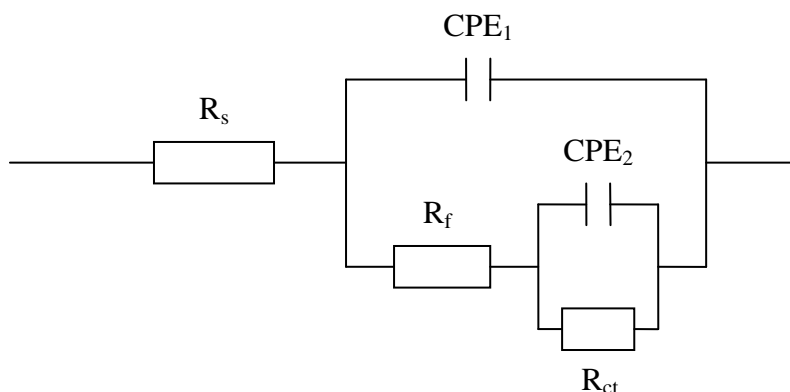

Figure 5. The equivalent circuit model used to fit the EIS experiment data

From Figure 4, two capacitive loops were noticed which could not be distinguished with the first loop characterized by a relative small loop in the high frequency range. The high frequency part represented the impedance of a surface adsorption layer and can be described as adsorption capacitance and adsorption resistance and the surface of the dielectric film has a smaller time constant. The low frequency part is associated with the Faradaic process occurring on the bare metal in the adsorbed inhibitor layer[29-31]. The capacitive loop is related to charge transfer in corrosion process[32-33], whereas the inductive loop might correlate to adsorption-desorption process of the inhibitive molecules on the electrode surface[21]. In this equivalent circuit shown in Figure 5, R_s represents the solution resistance, R_{ct} represents charge transfer resistance; constant phase element CPE_1 is composed of the membrane resistance R_f and n_1, CPE_2 is composed of double-layer capacitance C_{dl} and n_2 . The impedance function of the CPE is following[34]:

$$Z_{CPE} = Y^{-1}(j\omega)^{-n} \qquad (3)$$

where Y is a proportional factor, ω is the angular frequency, and the deviation parameter n is a valuable criterion of the nature of the metal surface which reflects microscopic fluctuations of the surface. The experimental results of EIS measurements obtained for the corrosion of mild steel with and without inhibitors are summarized in Table 4. The inhibition efficiencies obtained from electrochemical measurements are not the same with those calculated from weight loss measurement, but the trend is the same.

Table 3. Impedance data of mild steel in 3.5% NaCl in presence of different inhibitor concentrations

inhibitor	Content mg/L	R_s ($\Omega.cm^2$)	R_f ($\Omega.cm^2$)	R_{ct} ($\Omega.cm^2$)	CPE_1 ($F.cm^{-2}$)	n_1	CPE_2 ($F.cm^{-2}$)	n_2	IE (%)
blank	0	2.519	67.04	978.6	4.648×10^{-4}	0.77	4.699×10^{-3}	0.62	---
CSB	100	3.997	290.9	1669	7.236×10^{-4}	0.66	3.987×10^{-3}	0.49	41.37
	200	4.947	189.2	3596	2.450×10^{-4}	0.81	2.182×10^{-3}	0.52	72.79
	400	4.429	221.8	2180	1.595×10^{-4}	0.65	1.773×10^{-3}	0.57	55.11
	600	3.323	143.1	1968	2.147×10^{-4}	0.64	7.898×10^{-3}	0.36	50.27
	800	6.661	158.6	1586	2.220×10^{-4}	0.74	2.057×10^{-3}	0.34	38.74
CM-CSB	100	2.683	59.18	1541	1.364×10^{-3}	0.68	3.648×10^{-4}	0.74	36.50
	200	4.547	0.1201	2046	1.363×10^{-3}	0.61	4.233×10^{-5}	0.84	52.17
	400	2.156	7.25	2591	1.079×10^{-4}	0.72	2.284×10^{-4}	0.74	62.23
	600	1.479	9.225	3066	4.616×10^{-5}	0.78	2.2266×10^{-4}	0.70	68.08
	800	1.088	199.6	5605	1.115×10^{-4}	0.82	6.323×10^{-4}	0.59	82.54

From Table 3, R_{ct} values of the CSB on mild steel increased first and then decreased and the maxium value can be obtained at 200mg/L. This is probably because the inhibitor adsorbing on the surface is no longer stable. It is also cleared that this trend is same with that of charge transfer resistance R_{ct}. It also shows that the adsorbed film reduced the dielectric constant present on the metal surfaces. Effective corrosion resistance is associated with high R_{ct} and low C_{dl} values[35, 36]. In the case of two inhibitors, efficient adsorption is the results of some factors: π electrons of the aromatic system and double bonds, nitrogen and oxygen electronegative atoms[37]. But the difference in inhibition effect between the CSB and the CM-CSB may be the introduction of -COOH which increases its water-soluble and adsorption capacity on the mild steel surface. CSB is not well water-soluble, which are prone to desorption, so that inhibition efficiency decreases.

3.4 Corrosion morphology analysis

In order to evaluate the conditions of the mild steel surfaces in 3.5% NaCl solution, a superficial analysis was carried out. The SEM photographs are given in Fig.5
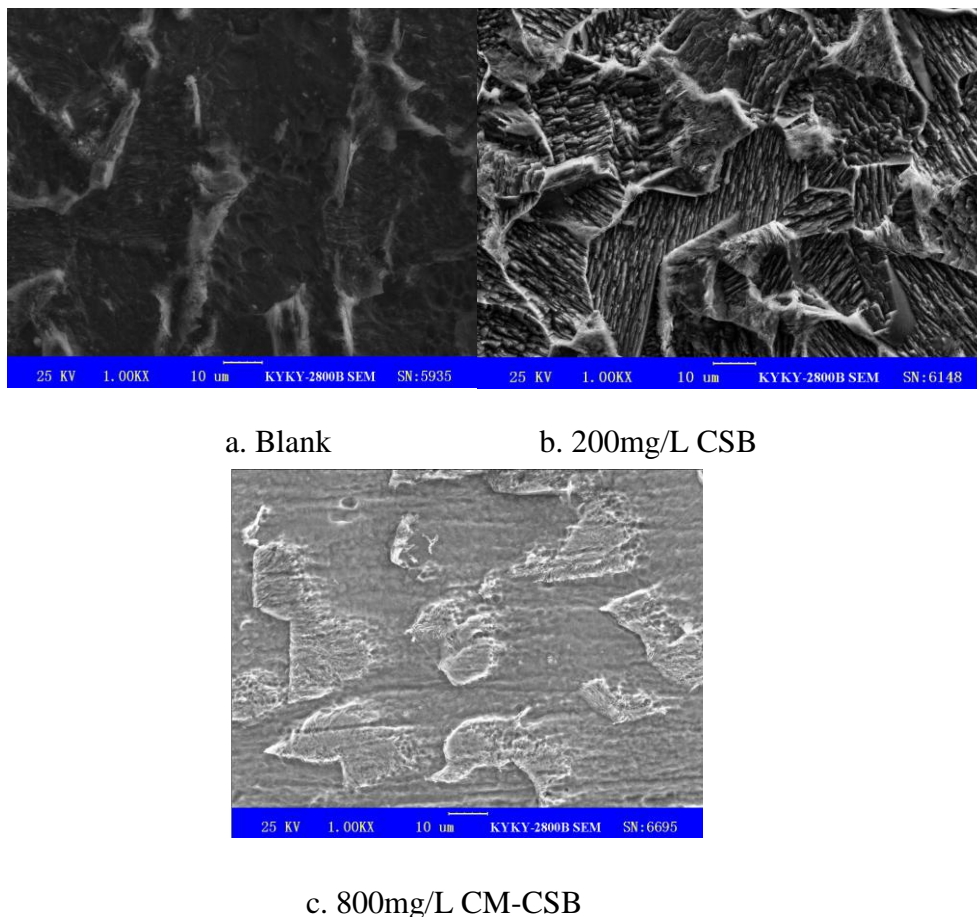
a. Blank   b. 200mg/L CSB

c. 800mg/L CM-CSB

Figure 6. SEM micrographs of mild steel after immersion in 3.5% NaCl (a) Blank; (b) 200mg/LCSB; (c) 800mg/L CM-CSB

Figure 6.a represents the surface morphology of the specimen in the absence of the inhibitor. It is obvious that the mild steel specimen severely corroded with many corrosion pits. In the case of 200mg/L CSB (Figure 6.b), the morphology is relatively smooth than that in blank, but it is more serious than that in 800mg/L CM-CSB as shown in Figure 6.c. It indicates that incomplete adsorption layer forms and protects the specimen surface from serious corrosion, so the corrosion of mild steel is lightly in comparison with that in blank. After addition of CM-CSB , the surface morphology of mild steel is smoother than that in CSB case suggesting that the inhibition ability is in the order of CM-CSB > CSB. This agrees with the results obtained from electrochemical measurement[38].

3.5 Adsorption isotherm

The interaction between the inhibitors and the mild steel surface can be provided by the adsorption isotherm. Because CM-CSB has better inhibition performance, its adsorption action was studied. It is assumed that organic molecules can absorb on the surface, therefore, the surface coverage θ equals to $IE_w\%$ as follows[39]:

$$\theta = \frac{W_0 - W}{W_0}$$

(6)

Hence, an attempt was made to test the Langmuir, Temkin, and Frumkin isotherms[40-42]. The langmuir isotherm was found to provide the best description of the adsorption behavior. The Eq. (7) and (8) are as follows:

$$\theta/(1-\theta) = k_{ads} \, C$$

(7)

$$k_{ads} = (1/55.5)\exp\left(-\Delta G^0_{ads}/RT\right)$$

(8)

Where C is the concentration of the inhibitor, k_{ads} represents adsorption equilibrium constant, ΔG^o_{ads} is the standard free energy of adsorption.
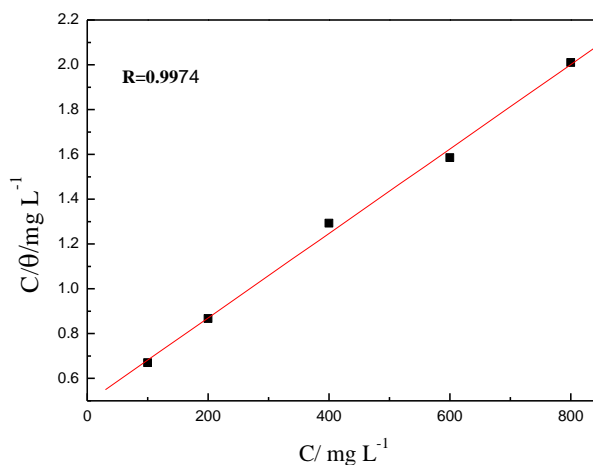
Figure 7. Langmuir adsorption isotherm of CM-CSB on mild steel in 3.5% NaCl solution

As shown in Figure 7, the correlation coefficient R of the straight line is 0.9974. The value for the Gibbs free energy of adsorption is -45.95 KJ/mol. Generally, the absolute value of ΔG^0_{ads} is higher than 40kJ/mol, the adsorption can be seen as chemisorption. Therefore, the adsorption of the CM-CSB is chemisorption and spontaneous in nature, which provides a comprehensive set of tools to perform atomistic simulations on complex systems[43].

3.6 Quantum chemical calculation

The effectiveness of an inhibitor depends on its spatial molecular structure and electronic structure[44, 45]. For further understanding the interactions between the inhibitor molecules and the carbon steel surface, quantum chemical calculation is performed[46]. Frontier molecular orbital theory

is useful in predicting the adsorption centers. The energy of the highest occupied molecular orbital (HOMO) E_{HOMO} is related with the electron donating ability of the molecule[47, 48]. High values of E_{HOMO} indicate a tendency for the molecule to donate electrons to appropriate acceptor molecules. The energy of the lowest unoccupied molecular orbital - E_{LUMO} indicates the ability of accepting electrons to molecule[49-51]. The optimized molecular monomer structure, the highest occupied molecular orbital (HOMO) and the lowest unoccupied molecular orbital (LUMO) is respectively shown in Figure 8. For HOMO of the molecule, it can be observed that the benzene ring and -C=N- have large electric density, while for the LUMO, -C-C- and –C=N- has large electron density; it suggested that the adsorption centre is on benzene ring and -C=N-. That is, the molecules can directly adsorb on the steel surface on the basis of donor-acceptor interactions between the electrons of the benzene ring, -C=N- and the vacant d-orbital of iron atoms[52, 53]. Moreover, it can be concluded that carboxymethylation don't play a direct role in inhibition effect, but improves the solubility of the inhibitors increasing the number of effective groups indirectly.
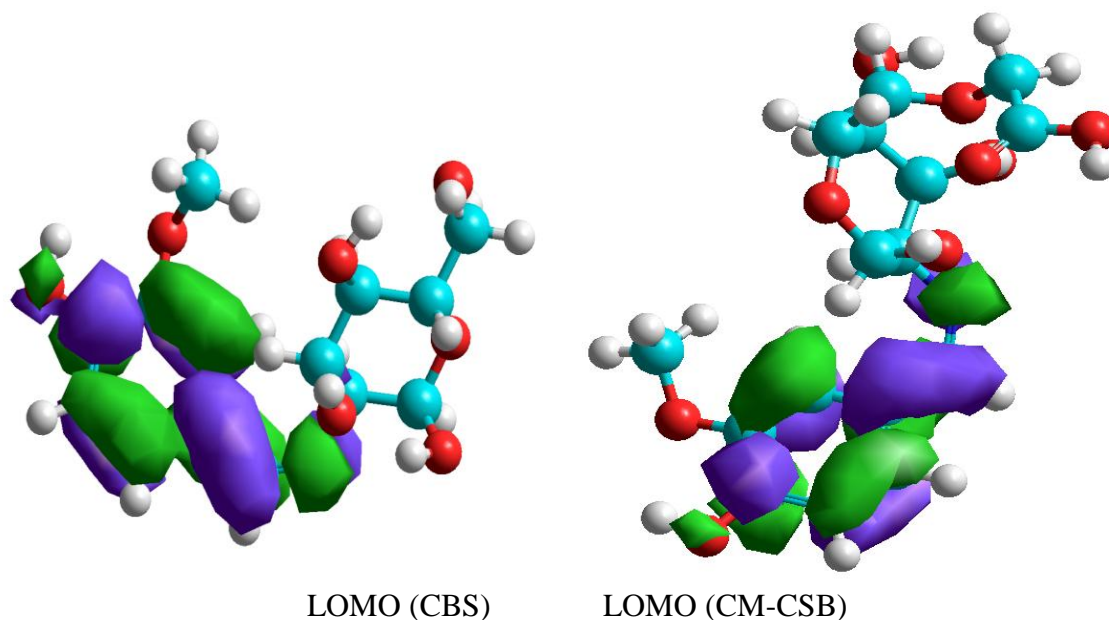

CSB   CM-CSB

HOMO (CBS)   HOMO (CM-CSB)

LOMO (CBS)   LOMO (CM-CSB)
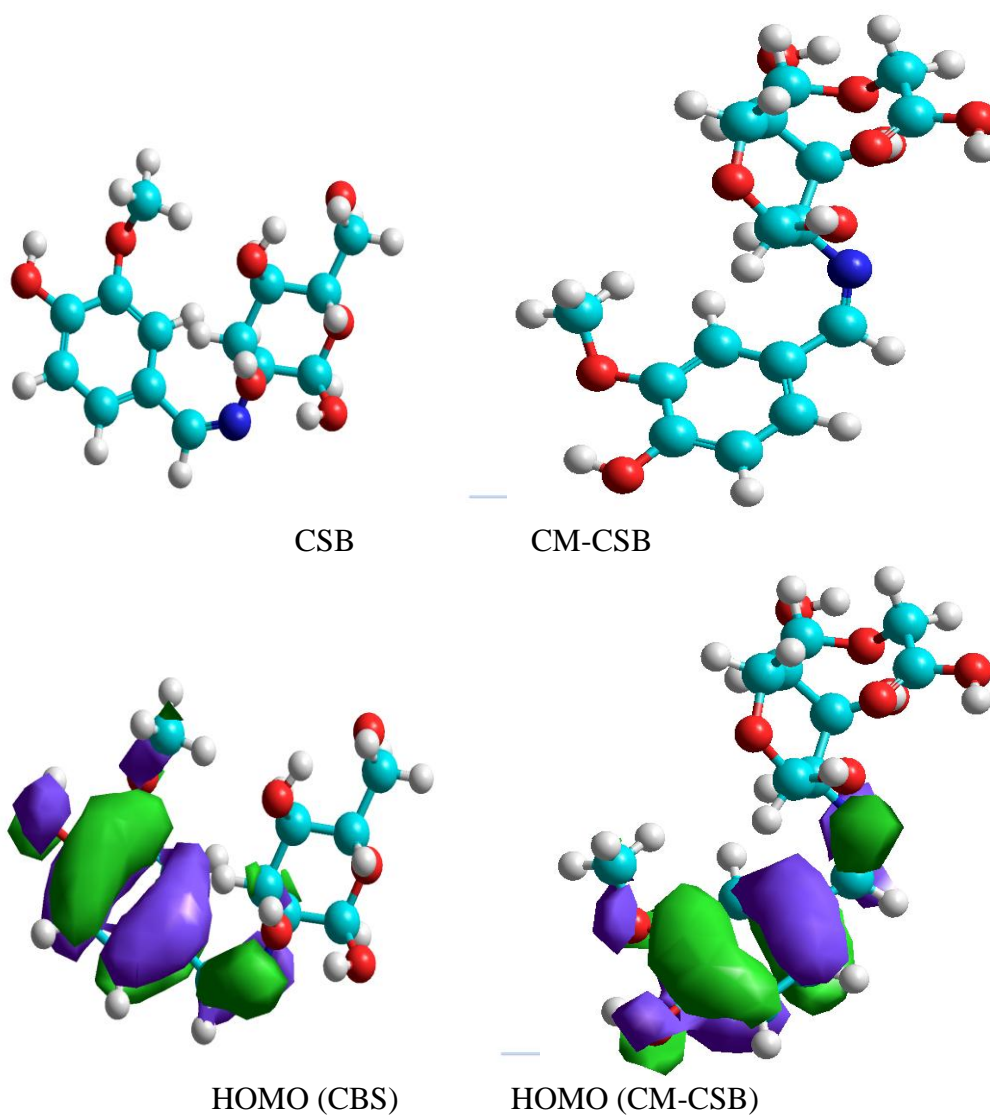
Figure 8. Molecular structure and frontier molecule orbital density distribution

4. CONCLUSIONS

1. The inhibition efficiency is in the order of CM-CSB > CSB. For CSB inhibition efficiency increases at first, then decreases with the increase inhibitor concentration and reaches the maximum at 200mg/L. While the CM-CSB's efficiency increases with the concentration and reaches the maximum at 800mg/L.

2. The CSB acts as a mixed type inhibitor and the CM-CSB acts as a cathode-based mixed corrosion inhibitor.

3. The adsorption of CM-CSB obeys the Langmuir isotherm at 298K. The negative values of ΔG_{ads}^{o} indicate that the adsorption of the CM-CSB is a spontaneous process, and the adsorption mechanisms is chemisorption in nature.

4. For CM-CSB, carboxymethylation improves its solubility thus increasing the number of effective groups indirectly.

References

1. J.I. Bregmann, *Corrosion Inhibitors*, P.T. Macmillan, New York, 1963.
2. N. Hackerman, Langmuir 3 (1987) 922.
3. C.C. Nathan, *Organic Inhibitors*, NACE, Houston, 1977.

4. M. Rinaudo, *Prog. Polym. Sci.* 31 (2006) 603.
5. S. Kim, N. Rajapakse, *Carbohyd. Polym.* 62 (2005) 357.
6. T. Sugama, M. Cook, Prog. Org. coat. 38 (2000) 79.
7. W. Morris, A. Vico, M.Vazquez, *Corros. Sci.* 44 (2002) 81.
8. B. Elsener, M. Buchler, F. Stalder, H. Bohni, Corros. 55 (1999) 1155.
9. B. Elsener, M. Buchler, F. Stalder, H. Bohni, *Corros.* 56 (2000) 727.
10. H. Saricimen , M. Mohammad, A. Quddus, M. Shameem, M.S. Barry, *Cement. Concrete. Comp.* 24 (2002) 890.
11. T.A. Söylev, M.G. Richardson, *Constr. Build. Mate.* 22 (2008) 609.
12. L. Y. Zheng, J. F. Zhu, *Carbohydr. Polym.* 54 (2003) 527.
13. F. Shahidi, J. K. V. Arachchi, Y. J. Jeon, *Sci. Technol.* 10 (1999) 37.
14. A.Yamada, N. Shibbuya, O. Kodamma, T. A.Katsuka, *Biosci. Biotechnol. Biochem.* 57 (1993) 405.
15. H. Shokry, M. Yuasa, I. Sekine, R.M. Issa, H.Y. El-Baradie, G.K. Gomma, *Corros. Sci.* 40 (1998) 2173.
16. S. Li, S. Chen, S. Lei, H. Ma, R. Yu, D. Liu, *Corros. Sci.* 41(1999) 1273.
17. K.C. Emregu, O. Atakol, *Mater. Chem. Phys.* 82 (2003) 188.
18. K.C. Emregu, O. Atakol, *Mater. Chem. Phys.* 83 (2004) 373.
19. K.C. Emregu, R. Kurtaran, O. Atakol, *Corros. Sci.* 45 (2003) 2803.
20. A. Asan, S. Soylu, T. Kıyak, et al. *Corros. Sci.* 48 (2006) 3933.
21. A. Yurt, S. Ulutas, H. Dal, *Appl. Surf. Sci.* 253 (2006) 919.
22. M. Kendig, S.Jeanjaquet, *J. Electrochem. Soc.* 149 (2002) B47.
23. F. Bentiss, M. Traisnel, L. Gengembre and M. Lagrenée, *Appl. Surf. Sci.* 152 (1999) 23.
24. W. D. Roberton, *J. Electrochem Soc,* 98(1951) 94.
25. Cao Chunan. *Corrosion electrochemistry.* Beijing: Chemical Industry Press.1990.
26. H. Ashassi-Sorkhabi, M.R. Majidi, K. Seyyedi, *Appl. Surf. Sci.* 225 (2004) 176.
27. S.S.A. El-Rehim, A.M.M. Ibrahim, K.F. Khaled, *J Appl Electrochem* 29(1999) 593.
28. S.S. Abdel-Rehim, A.M. Magdy, K.F. Khaled, *Mater. Chem. Phys.* 70(2001) 268.
29. I.D. Raistrick, *Electrochim. Acta* 35 (1990) 1579.
30. H.A. Sorkhabi, S.A. Nabavi-Amri, *Electrochim. Acta,* 47 (2002) 2239.
31. H.A. Sorkhabi, T.A. Aliyev, S. Nasiri, R. Zareipoor, *Electrochim. Acta* 52 (2007) 5238.
32. H. Ashassi-Sorkhabi, N. Ghalebsaz-Jeddi, F. Hashemzadeh, H. Jahani, *Electrochim. Acta* 51 (2006) 3848.
33. A.Popova, E.Sokolova, S.Raicheva, M.Christov, *Corros Sci,* 45 (2003) 33.
34. F.M. Al Kharafi, I.M. Ghayad, R.M. Abdullah, *Int. J. Electrochem. Sci.* 7 (2012) 3289.
35. F. Bentiss, M. Traisnel, M. Lagrenee, *Corros. Sci.* 42 (2000) 127.
36. M. Scendo, D. Poddebniak, J. Malyszko, *J. Appl. Electrochem.* 33 (2003) 287.
37. M. Behpour, S.M. Ghoreishi, *Mater. Chem. Phys.* 107 (2008) 153.
38. P. Zhao, Q. Liang, Y. Li, Electrochemical, *Appl. Surf. Sci.* 252 (2005) 1596.
39. M. Bouklah, B. Hammouti, M. Lagrenee, F. Bentiss, *Corro. Sci.* 48 (2006) 2831
40. K.C. Emregul, O. Atakol, *Mater. Chem. Phys.* 82 (2003) 188.
41. M.R. Arshadi, M.G. Hosseini, M. Ghorbani, *Br. Corros. J.* 37 (2002) 76
42. A. Popova, M. Christov, S. Raicheva, E. Sokolova, *Corros. Sci.* 46 (2004) 1333.
43. K.F. Khaled. *Mater. Chem. Phys.* 112 (2008) 104.
44. A.Y. Musa, R.T.T. Jalgham, A.B. Mohamad, *Corros. Sci.* 56 (2012) 176.
45. S. Xia, M. Qiu, L. Yu, F. Liu, H. Zhao, *Corros. Sci.* 50 (2008) 2021.
46. M. Finšgar, A. Lesar, A. Kokalj, I. Milošev, *Electrochim. Acta* 53 (2008) 8287.
47. K.F. Khaled, *Electrochim. Acta* 53 (2008) 3484.
48. G. Gece, *Corros. Sci.* 50 (2008) 2981.
49. E. Machnikova, K.H. Whitmire, N. Hackerman, *Electrochim. Acta* 53 (2008) 6024.
50. I.B. Obot, N.O. Obi-Egbedi, Corros. Sci. 52 (2010) 198.

51. H. Ashassi-Sorkhabi, B. Shaabani, D. Seifzadeh, *Electrochim. Acta* 50 (2005) 3446.
52. C. Wang, S. Chen, H. Ma, *J. Appl. Electrochem.* 33 (2003) 179.
53. A. Lalitha, S. Ramesh, S. Rajeswari, *Electrochim. Acta* 51 (2005) 47.